

Laser remote sensing in highly turbid waters: validity of the lidar equation

Stefan Harsdorf and Rainer Reuter

Carl von Ossietzky Universität Oldenburg, Fachbereich Physik, 26111 Oldenburg, Germany

ABSTRACT

A submarine fluorescence lidar has been developed for the detection of hazardous chemicals on the seafloor of the German Bight. Signals are dependent on the inherent optical properties of the seawater column, the seabed and the substance properties, mainly their absorption coefficient, volume scattering function, fluorescence quantum yield and reflectance. Although the instrument is designed to inspect the seafloor it allows to record time-resolved spectra in order to derive information about the water column.

Interpretation of these data is normally done with the classical lidar equation which is based on several simplifying assumptions. In its conventional analytical form multiple scattering is not considered. This leads to an increase in signal intensity and to optical ringing. Additionally, fluorescence lifetimes and detector response function may result in an uncertainty of distance determination.

Monte Carlo simulations were done to analyse the performance of the submarine fluorescence lidar for realistic scenarios. Results are compared with theoretical predictions of the lidar equation. It is shown that the error in signal intensity increases with the turbidity whereas the slope of the lidar curve appears to be independent of it. Depth-resolved measurements are not limited by the penetration depth of the light but by multiple scattering effects.

Keywords: lidar, lidar equation, Monte Carlo, single scattering, multiple scattering

1 INTRODUCTION

A fluorescence lidar has been presented which was designed for underwater operation in the German Bight.¹ Illumination source of this sensor is a Nd:YAG laser with 70 mJ pulse energy at 355 nm. Although this lidar is operated to detect hazardous substances on the seafloor, the sampling rate of 250 MHz provides an analysis of the water column with a maximum distance resolution of about 0.2 m. Lidar signals are usually interpreted with the help of equations which are based on several simplifications. It is mostly assumed that a single photon interacts only once with the surrounding medium, and the measurement process is regarded as ideal. Temporal dilations and decay times during the induction of photons are also neglected.

2 LIDAR EQUATION

Regarding a pulsed monostatic lidar, the energy $\Delta E(\lambda, R)$ collected by the detector within the wavelength interval $(\lambda, \lambda + \Delta\lambda)$ and the depth interval $(R, R + \Delta R)$ can be given in its most general form²

$$\Delta E(\lambda, R) \equiv E(\lambda, R) \Delta R \Delta \lambda = \eta(\lambda) \cdot \frac{A_r}{R^2} \cdot g(R) \cdot T(\lambda, R) \cdot W(\lambda, R) \Delta R \Delta \lambda \quad (1)$$

η is the spectral transmission of the detector, $T(\lambda, R)$ the transmission in the medium over the range R at wavelength λ . Transmission has no physical dimension. A_r is the effective aperture of the detection optics. The ratio of A_r and R^2 describes the solid angle, which is formed by the lidar detector from the distance R . Its unit is steradian. The quantity $W(\lambda, R)$ describes the energy of the induced radiation at depth R in units $\text{J sr}^{-1} \text{m}^{-1} \text{nm}^{-1}$. The product $W(\lambda, R) \Delta R \Delta \lambda$ is therefore the radiation induced in the depth interval $(R, R + \Delta R)$ and in the wavelength interval $(\lambda, \lambda + \Delta \lambda)$ in J sr^{-1} . The dimensionless geometric form factor is the probability of recording a photon which is induced at a distance R and hits the detector. Furthermore, the fundamental lidar relationship holds:

$$R = \frac{c_w \cdot t}{2} \quad (2)$$

and hence

$$\Delta R = \frac{c_w \cdot \Delta t}{2}$$

Δt corresponds to the temporal resolution of the sensor. From eq. 1 it follows

$$\begin{aligned} E_{\lambda}(R) &\equiv E(\lambda, R)\Delta R = \eta(\lambda) \cdot s(R) \cdot T(\lambda, R) \cdot W(\lambda, R)\Delta R \\ &= \eta(\lambda) \cdot s(R) \cdot T(\lambda, R) \cdot W(\lambda, R) \frac{c_w \cdot \Delta t}{2} \end{aligned} \quad (3)$$

with the sensitivity function

$$s(R) := g(R) \frac{A_r}{R^2} .$$

$s(R)$ has the unit sr, $E_{\lambda}(R)$ the unit $J \text{ nm}^{-1}$. The transmission $T(\lambda, R)$ over distance R is given by the attenuation coefficient $c(\lambda, R)$ and Lambert-Beer's law

$$T(\lambda, R) = e^{-\int_0^R c(\lambda, r) dr} .$$

In case of elastic backscattering the induced energy $W(\lambda, R)$ is determined with the approximation $R^2 \gg A_r$ by

$$W(\lambda, R) = E_1 \cdot e^{-\int_0^R c_L(\lambda_L, r) dr} \cdot \beta(\pi, \lambda, R) ,$$

where the volume scattering function β can be interpreted as differential cross section per volume unit, per solid angle and wavelength. E_1 is the laser pulse energy. This leads to the single scattering lidar equation in its form which describes the collected energy in the time intervall $(t, t+\Delta t)$.

$$E_{\lambda}(t = \frac{2R}{c_w}) = \eta(\lambda_1) \cdot s(R) \cdot E_1 \cdot \beta(\pi, \lambda_1, R) \cdot \frac{c_w \cdot \Delta t}{2} \cdot e^{-2 \int_0^R c(\lambda_1, r) dr} \quad (4)$$

Eq. 4 implies that the laser pulse duration τ_1 is much shorter than Δt . Temporal dilatations such as the detector pulse response time remain unconsidered. If the average laser pulse power $P_1 = E_1 \tau_1$ is taken into account, the single scattering lidar equation can be written in a form which describes the radiaton flux $P_{\delta}(\lambda, t) = E_{\lambda}(t) \Delta t$ detected by the receiver at time $t = 2R c_w^{-1}$ in $W \text{ nm}^{-1}$ as

$$P_{\delta}(\lambda_1, t) = \eta(\lambda_1) \cdot s(R) \cdot P_1 \cdot \beta(\pi, \lambda_1, R) \cdot \frac{c_w \cdot \tau_1}{2} \cdot e^{-2 \int_0^R c(\lambda_1, r) dr} . \quad (5)$$

If the laser pulse duration $P_1(t)$ and pulse response function $R_r(t)$ of the detector are not much shorter than the temporal resolution Δt of the lidar, then the signal will be blurred. This means, that photons induced at the same depth R are no longer detected at the same time t . Eq. 2 is no longer valid. Mathematically this can be described by a convolution integral. The measured lidar signal $P(t)$ is then written as

$$P(t) = P_{in}(t) \times R_m(t) \times P_{\delta}(t)$$

with $P_{in}(t)$ and $R_m(t)$ as symbols for normalized functions of $P_1(t)$ and $R_r(t)$, respectively, and where the symbol \times denotes the convolution. The convolution of $P_{in}(t)$ and $R_m(t)$ can be condensed to one system function $S_{sys}(t)$, and the convolution equation simplifies to

$$P(t) = S_{sys}(t) \times P_{\delta}(t) . \quad (6)$$

Deconvolution techniques that can be used to extract $P_{\delta}(t)$ from eq. 6 in the presence of noise will be presented elsewhere.³ Eq. 5 does not take into account multiple scattering effects.

3 MONTE CARLO SIMULATIONS

A simple variance reducing Monte Carlo technique is used to calculate the sensitivity function $s(R)$ of the lidar. According to the single scattering lidar equation, the sensitivity function $s(R)$ corresponds to the lidar signal of a medium with an attenuation of 0 m^{-1} and an isotropic backscatter coefficient $\beta(R) = (4\pi)^{-1} \text{ sr}^{-1}$ at the excitation wavelength. If multiple scattering is excluded, only scattering angles within the solid angle $\Omega(z)$ defined by the detector are allowed. In accordance with this, the weight of a photon is $\Omega(z) (4\pi \text{ sr})^{-1}$. The result is normalized to the total number of photons per $4\pi \text{ sr}$.

Fig. 1 shows the sensitivity function of the lidar.¹ Monte Carlo simulations were done to examine the performance of the lidar in different waters and to investigate the effect of multiple scattering. The inherent optical properties of the water column which are needed as input data were taken from the literature,⁴ which include clear ocean water, offshore water with medium turbidity, and highly turbid coastal water. The results of his measurements are seen in Table 1 and Fig. 2.

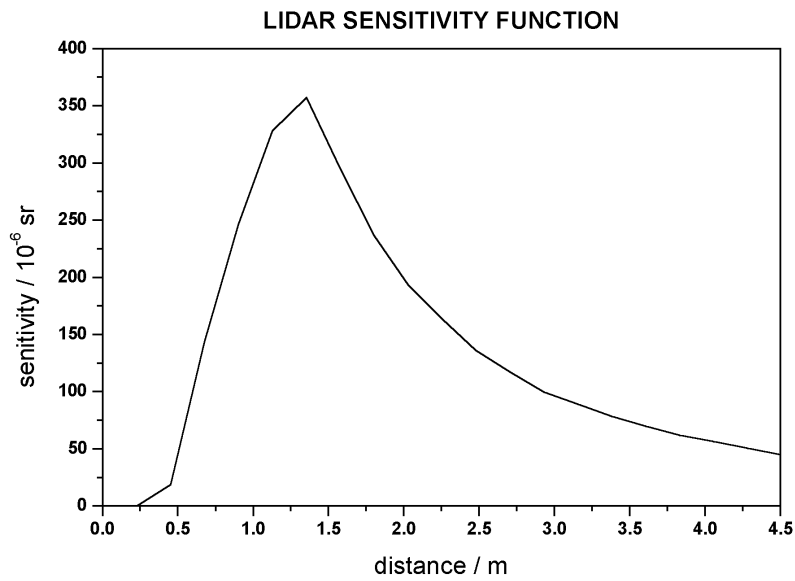


Fig. 1: Sensitivity function $s(R)$ of the submarine lidar

	a / m^{-1}	b / m^{-1}	c / m^{-1}	$\omega=b/c$
San Diego Harbor	0.366	1.824	2.190	0.8329
Offshore Southern California	0.179	0.219	0.398	0.5503
Tongue of the Ocean	0.114	0.037	0.151	0.2450

Table 1: Absorption coefficient a , scattering coefficient b , attenuation coefficient c and single scattering albedo ω at $\lambda=514$ nm of three water types.⁴

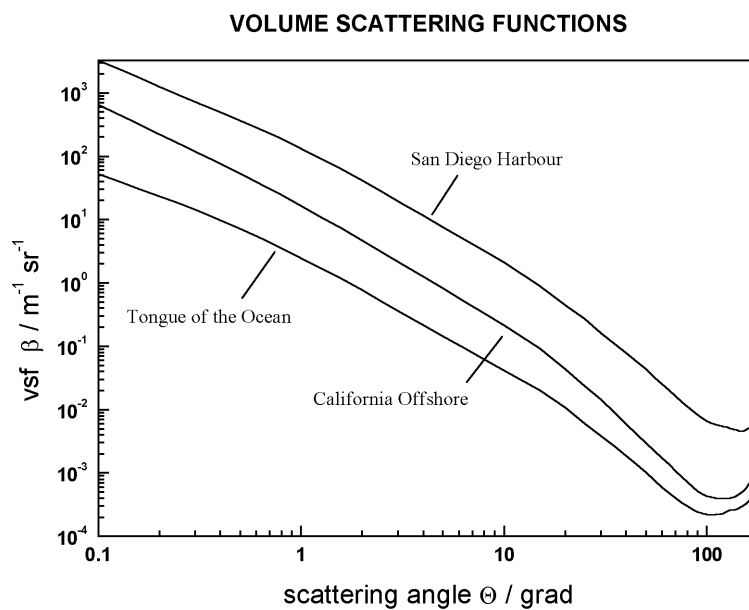


Fig. 2: Volume scattering functions of selected waters.⁴

For the simulations, the scattering coefficient is set to be independent of the wavelength.⁵ Absorption is assumed to be influenced by yellow substance only, with a characteristic spectrum of the absorption coefficient.⁶

$$a(\lambda) = a(532\text{nm}) \cdot e^{-0.014(\lambda-532\text{nm})} \quad (7)$$

Based on the known sensitivity function, the lidar signal of yellow substance fluorescence at 450 nm can be calculated.

$$E_{450\text{nm}}(R) = k \cdot \eta(450\text{nm}) \cdot s(R) \cdot T(450\text{nm}, R) \cdot W(450\text{nm}, R) \frac{c_w \cdot \Delta t}{2} \quad (8)$$

with

$$k = \frac{1 - e^{-(c(355\text{nm})+c(450\text{nm})) \cdot \Delta R}}{(c(355\text{nm}) + c(450\text{nm})) \cdot \Delta R}$$

$$W(450\text{nm}, R) = E_1 \frac{q_{ys}(450\text{nm}, 355\text{nm}) \cdot a(355\text{nm})}{4\pi \text{ sr}} e^{-c(355\text{nm}) \cdot R}$$

and

$$T(450\text{nm}, R) = e^{-c(450\text{nm}) \cdot R}$$

The factor k is a correction due to the fact that ΔR is not infinitively small. The fluorescence decay time of yellow substance is about 2 ns, and therefore not considered in the analytical approach and the computer simulations. The Monte Carlo experiments are done with a laser pulse energy of 5 million photons at 355 nm. Detection wavelength is 450 nm, with an assumed fluorescence quantum yield $q_{ys}(450\text{nm}, 355\text{nm})=1 \text{ nm}^{-1}$ of yellow substance in order to minimize computation time. A realistic value for $q_{ys}(450\text{nm}, 355\text{nm})$ would be about 0.0001 nm^{-1} .⁷ The refractive index of seawater is set to 1.33.

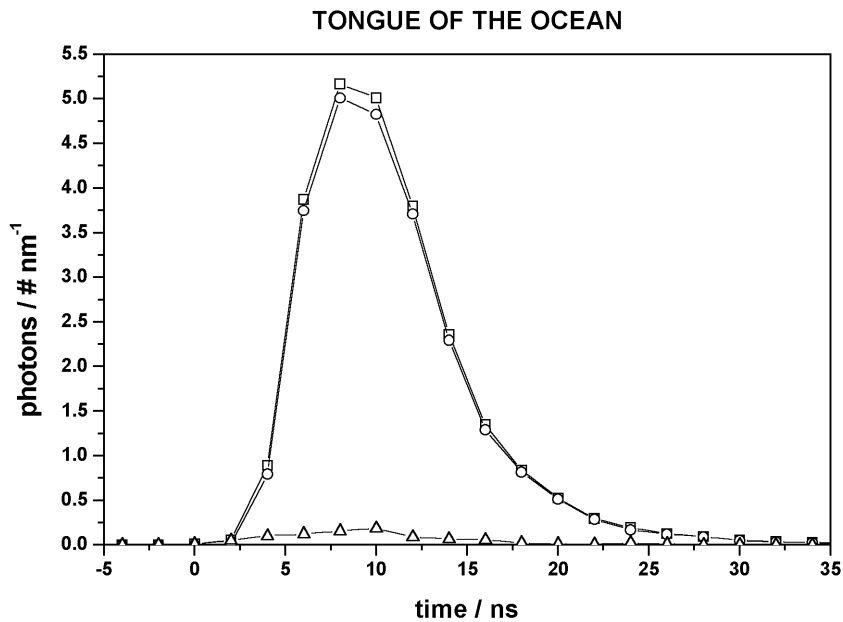


Fig. 3: Simulated lidar signal for Tongue of the Ocean water. Squares: total signal; circles: single scattering; triangles: multiple scattering.

Fig. 3 shows the simulated lidar spectra of the „Tongue of the Ocean“ water type. The lidar signal of Offshore Southern California water is shown in Fig. 4. Although multiple scattering has increased when compared with the clear ocean water signal, single scattering is still the main part of the signal. Fig. 5 displays the result of the simulation for San Diego Harbor water. The single scattering part nearly disappears compared to the multiple scattering component. The increase of intensity by multiple scattering is mainly found in the near-field.

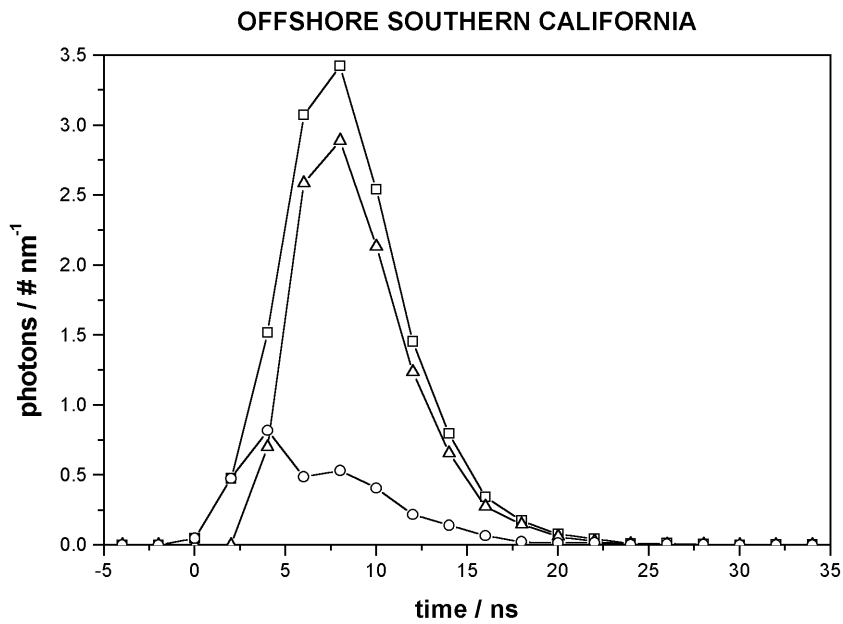


Fig. 4: Simulated lidar signal for Offshore Southern California water. Squares: total signal; triangles: single scattering; circles: multiple scattering.

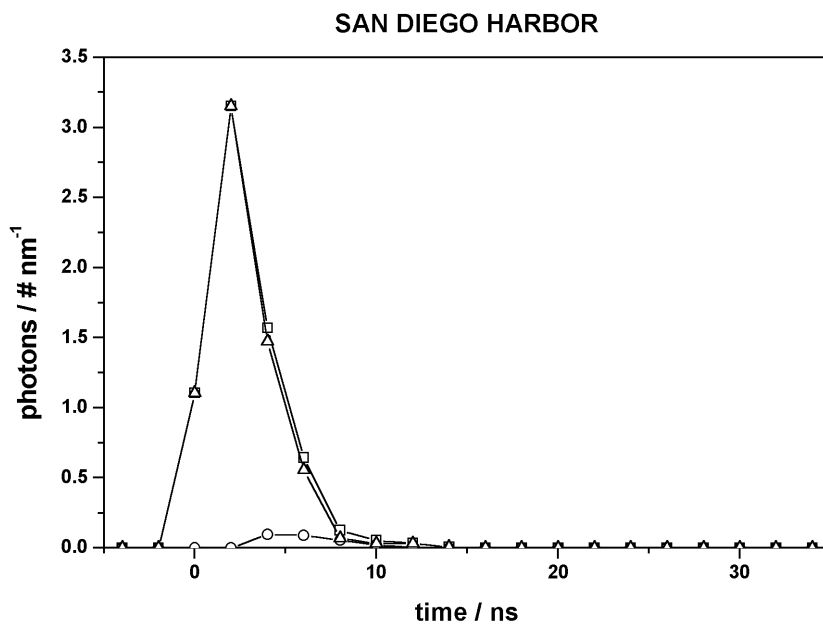


Fig. 5: Simulated lidar signal for San Diego Harbor water. Squares: total signal; circles: single scattering; triangles: multiple scattering.

Solving eq. 8 with regard to the data given in Table 1 yields the signals shown in Fig. 6.

Table 2 lists the average errors between the simulated lidar signals and the theoretically predicted signals, normalized to the maxima of the theoretically calculated curves. Total signal intensity and the single scattering component are treated separately. The single scattered parts of the signals show good agreement with the theory. The errors are acceptable small and due to the random nature of Monte Carlo simulations. Regarding the total signal power the error grows with increasing turbidity up to 285 % for the San Diego Harbor water. For it is not possible to separate the single scattering component from the total lidar signal, these errors are the relevant ones in lidar measurements.

	total signal intensity	single scattering component
San Diego Harbor	285.421 %	3.292 %
Offshore Southern California	4.255 %	0.805 %
Tongue of the Ocean	2.025 %	2.495 %

Table 2: Normalized average intensity errors between MC simulations and theory

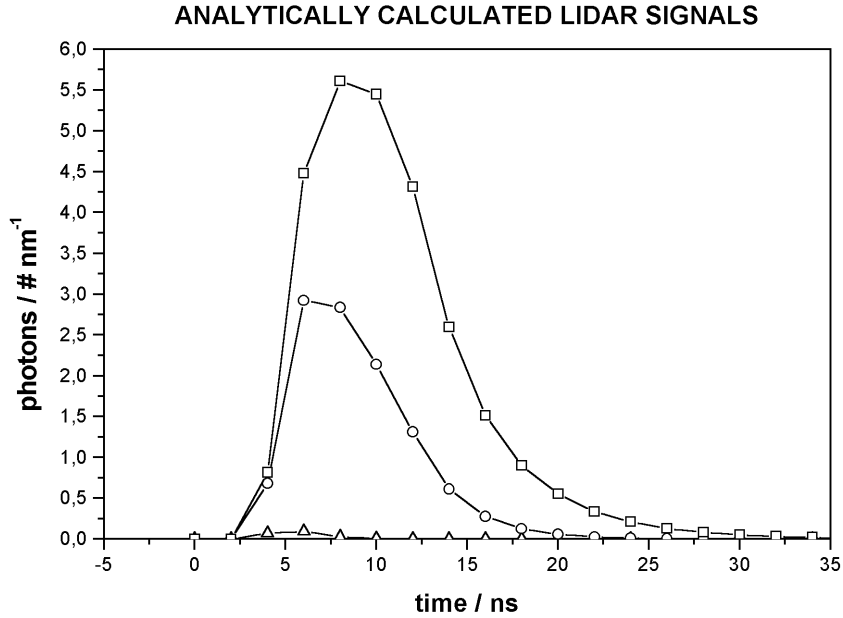


Fig. 6: Analytically calculated signals. Squares: Tongue of the Ocean; circles: Offshore Southern California; triangles: San Diego Harbor.

4 INVERSION OF LIDAR SIGNALS

Starting from eq. 5 the normalized logarithmic lidar signal $S(\lambda, t)$ can be defined as

$$S(\lambda, t) := \ln \left(\frac{1}{s(R)} \cdot P_{\delta}(\lambda, t) \right) . \quad (9)$$

The convenient differential equation is

$$\frac{d}{dR} S(\lambda_1, R = \frac{c_w \cdot t}{2}) = \frac{1}{\beta(\pi, \lambda_1, R)} \cdot \frac{d}{dR} \beta(\pi, \lambda_1, R) - 2 \cdot c(\lambda_1, R) . \quad (10)$$

For a homogeneous water column eq. 10 simplifies to

$$\frac{d}{dR} S(\lambda_1, R = \frac{c_w \cdot t}{2}) = -2 \cdot c(\lambda_1, R) . \quad (11)$$

Regarding the fluorescence lidar signals, eq. 11 transforms to

$$\frac{d}{dR} S(\lambda_1, R = \frac{c_w \cdot t}{2}) = -(c(355\text{nm}) + c(450\text{nm})) \equiv -c_{2\text{paths}}(355\text{nm}, 450\text{nm}) , \quad (12)$$

introducing the two paths lidar attenuation coefficient $c_{2\text{paths}}$.

In Table 3 the values of $c_{2\text{paths}}$ derived from the MC signals can be seen together with their relative error compared to the input values. The high errors of the signal simulated for the San Diego Harbor water are due to the low signal-to-noise ratio. In contrast to the intensity, the errors in the slope do not vary significantly regarding the total signal and the single scattering component. This confirms the results of H. Gordon who solved the radiative transfer function of an airborne backscatter lidar numerically by Monte Carlo simulations in order to examine the

influence of multiple scattering.⁸ He found an exponential decay in sensitivity corrected lidar signals of homogeneous water bodies over four attenuation lengths.

	input data	analyt. solution / relative error	MC single scatter / relative error	MC total signal / relative error
San Diego Harbor	7.935 m ⁻¹	7.935 m ⁻¹ 0 %	6.671 m ⁻¹ - 15.9 %	6.940 m ⁻¹ - 12.5 %
Offshore Southern California	2.535 m ⁻¹	2.535 m ⁻¹ 0 %	2.653 m ⁻¹ + 4.7 %	2.478 m ⁻¹ - 2.2 %
Tongue of the Ocean	1.409 m ⁻¹	1.409 m ⁻¹ 0 %	1.385 m ⁻¹ - 1.7 %	1.389 m ⁻¹ - 1.4 %

Table 3: Two paths lidar attenuation coefficients

5 CONCLUSIONS

The lidar signal power is thought to be a direct measure of the concentration of substances such as yellow substance, whereas the slope of the time-resolved curve is used to derive the two paths lidar attenuation coefficient. The simulations showed that it is not possible to interpret the recorded signal intensity in high turbid waters with the conventional lidar equation because the multiple scatter component cannot be neglected. In comparison to it, the influence of multiple scattering on the derivation of attenuation coefficients appears to be less significant. In other words, multiple scattering strongly influences the intensity of a lidar signal, but not its temporal curve.

The performance of a depth resolved lidar with regard to quantitative fluorescence measurements is not limited by its penetration depth but by multiple scattering effects. Future research should focus on the formulation of a convenient lidar equation.

6 ACKNOWLEDGEMENTS

This study is supported with a grant of the Ministry of Research and Technology (BMBF), Germany, through the DLR Project Executive Department Environmental Protection and Technologies, Bonn.

7 REFERENCES

- ¹ S. HARSDORF, M. JANSSEN, R. REUTER, AND B. WACHOWICZ, "Design of an ROV-based lidar for seafloor monitoring", SPIE Vol. 3101 Remote Sensing of Vegetation and Water, and Standardization of Remote Sensing Methods, 288-297, 1997
- ² R. M. MEASURES, "Lidar equation analysis allowing for target lifetime, laser pulse duration, and detector integration period", Appl. Opt., Vol. 16, No. 4, 1092-1103, 1977
- ³ S. HARSDORF AND R. REUTER, "Stable deconvolution of noisy lidar signals", manuscript in preparation, 1999
- ⁴ T. J. PETZOLD, "Volume scattering functions for selected ocean waters", in: J.E. Tyler, "Light in the sea", John Wiley & Sons, 152-174, 1977
- ⁵ S. Q. DUNTLEY, "Light in the sea", J. Opt. Soc. Am., Vol. 53, 214-233, 1963
- ⁶ A. BRICAUD, A. MOREL, AND L. PRIEUR, "Absorption by dissolved organic matter of the sea (yellow substance) in the UV and visible domains", Limnol. Oceanogr. 26, 43-53, 1981
- ⁷ S. K. HAWES, K. L. CARDER, AND G. R. HARVEY, "Quantum fluorescence efficiencies of fulvic and humic acids: effects on ocean color and fluorometric detection", SPIE Vol. 1750 Ocean Optics XI, 212-223, 1992
- ⁸ H. R. GORDON, "Interpretation of airborne oceanic lidar: effects of multiple scattering", Appl. Opt., Vol. 21, No.16, 2996-3001, 1982